

Porphyrin-based colorimetric sensing of perfluorooctanoic acid as a proof of concept for perfluoroalkyl substance detection

Chloe M. Taylor,^a Theo A. Ellingsen,^a Michael C. Breadmore^b and Nathan L. Kilah^{a*}

^a Chemistry, School of Natural Sciences, University of Tasmania, Hobart, Tasmania, 7001, Australia.

E-mail: nathan.kilah@utas.edu.au

^b Australian Centre for Research on Separation Science (ACROSS), Chemistry, School of Natural Sciences, University of Tasmania, Hobart, Tasmania, 7001, Australia.

S1– Synthesis and General Methods

Synthetic Procedures: $\alpha,\alpha,\alpha,\alpha$ -5,10,15,20-Tetrakis(2-aminophenyl)porphyrin (1 eq) and anhydrous pyridine (4.2 eq) were combined in dry dichloromethane (5 mL) and stirred at room temperature for an hour in the absence of light. A solution of pentadecafluorooctanoyl chloride (4.2 eq) in dry dichloromethane (10 mL) was added dropwise. The mixture was magnetically stirred in the dark overnight at room temperature. Dichloromethane (5 mL) was added. The mixture was washed with water (20 mL), aqueous HCl (0.1 M, 20 mL) and saturated aqueous NaHCO_3 (20 mL). The organic phase was dried using Na_2SO_4 and filtered through a glass frit. The solvent was removed using rotary evaporation in the absence of heat and light to yield a dark crystalline purple material. The crude product was purified using column chromatography (silica gel, petroleum ether/acetone/dichloromethane, 4:1:1). Crystals suitable for x-ray diffraction were grown by slow evaporation from hexane. Crystals were dried under high vacuum. Single crystal X-ray crystallographic data have been deposited at the Cambridge Crystallographic Data Centre under deposition number CCDC 2080882 and can be accessed at <https://www.ccdc.cam.ac.uk/structures/> (Yield ~ 60%). ^1H NMR (CDCl_3) δ 8.79 (s, 8H), 8.65 (d, J = 8.46 Hz, 4H), 7.94 (m, 8H), 7.79 (s, 4H), 7.64 (t, J = 7.44 Hz, 4H), -2.68 (s, br, 2H). ^{13}C NMR (CDCl_3) δ 145.8, 136.6, 132.0, 129.2, 126.9, 125.6, 110.1, 25.6, 7.01. ^{19}F NMR (CDCl_3) δ -80.8, -118.9, -121.6, -121.2, -122.7 (two peaks coincide), -126.1. MS (FTMS + pESI): m/z for $\text{C}_{76}\text{H}_{31}\text{F}_{60}\text{N}_8\text{O}_4$ calcd 2259.1505, found 2259.1404.

Synthesis of tetrabutylammonium perfluorooctanoate salt (TBAPFO): This methodology was modified from a literature procedure.¹ Perfluorooctanoic acid (5×10^{-4} mol) is dissolved in warm deionized water with vigorous stirring. The solution is left to cool to room temperature before tetrabutylammonium hydroxide solution is added dropwise. The aqueous phase is extracted with dichloromethane, and the solvent is removed to yield a white solid. The solid product is twice recrystallized from dichloromethane via the addition of diethyl ether. ^1H NMR (CDCl_3) δ 3.28 (m, 8H), 1.65 (m, 8H), 1.43 (m, 8H), 1.00 (t, J = 7.32 Hz, 12H). ^{19}F NMR (CDCl_3) δ -80.8, -116.3, -122.3, -123.0, -123.9, -127.6.

General equipment and sampling considerations: Ideal materials to be used when preparing PFAS samples include polypropylene, high density polyethylene, PVC, stainless steel, and silicone. Some analysis methods require the use of materials that may adsorb PFAS (primarily glass). Glassware use was limited when possible, and it was acknowledged that it could have a minor impact on the effective PFAS concentration during analysis. Glassware that contained PFAS material was not reused throughout experiments. Materials that must be avoided to limit PFAS contributions to analysis include low density polyethylene and polytetrafluoroethylene (Teflon).

General method of UV-Visible titration: Path length of the quartz cell was 1 cm. For UV-visible titrations, a stock solution of **1** was prepared (2.2×10^{-3} M) in dichloromethane and serially diluted to required concentrations. Working solutions of TBA anion salts were prepared in the same manner. Host – guest titrations used solutions of guest prepared in the working concentration of host solution, according to literature methodologies.²

General method for aqueous “shake” extractions: Solutions of **1** dissolved in dichloromethane were combined with aqueous solutions of perfluorooctanoic acid. The vials are capped and agitated. The organic phase is collected for UV-visible spectroscopic analysis. Small extractions could be performed in polypropylene centrifuge tubes.

Soil spiking and sample preparation procedures: Soil was collected in large quantities (~1 kg) from the first 15 cm of soil in a public area using a stainless-steel spatula and a polypropylene container. The soil was subdivided into 250 g portions and dried in an oven at 40°C overnight. Solutions of PFOA in dichloromethane were prepared in volumetric flasks and applied to weighed amounts of dirt stored in polypropylene containers. The control sample was prepared by combining the same amount of dirt and volume of dichloromethane. The containers were agitated and left to evaporate. Once dry, the soil was again shaken to mix thoroughly before being used in extractions.³⁻⁵

S2– NMR Spectroscopy

NMR experiments were performed on a Bruker Avance III NMR spectrometer operating at 600 MHz (^1H), 150 MHz (^{13}C) or 564 MHz (^{19}F). The deuterated solvent used was CDCl_3 or CD_3OD , and chemical shifts were recorded in ppm. Spectra were calibrated by reference to the residual solvent peak at δ_{H} 7.26 and δ_{C} 77.16 ppm for CDCl_3 , and δ_{H} 4.78 and δ_{C} 49.15 ppm for CD_3OD . Coupling constants (J) were recorded in Hz. NMR spectra were run at low concentrations of **1**, as aggregation of the molecule increased the number of resonances, making assignment difficult. The sample was dried under high vacuum yet showed residual petroleum ether resonances. Single crystal X-ray crystallographic data showed the product cocrystallized with hexane, which suggests that the residual petroleum ether resonances visible in the ^1H NMR spectra are likely due to cocrystallization.

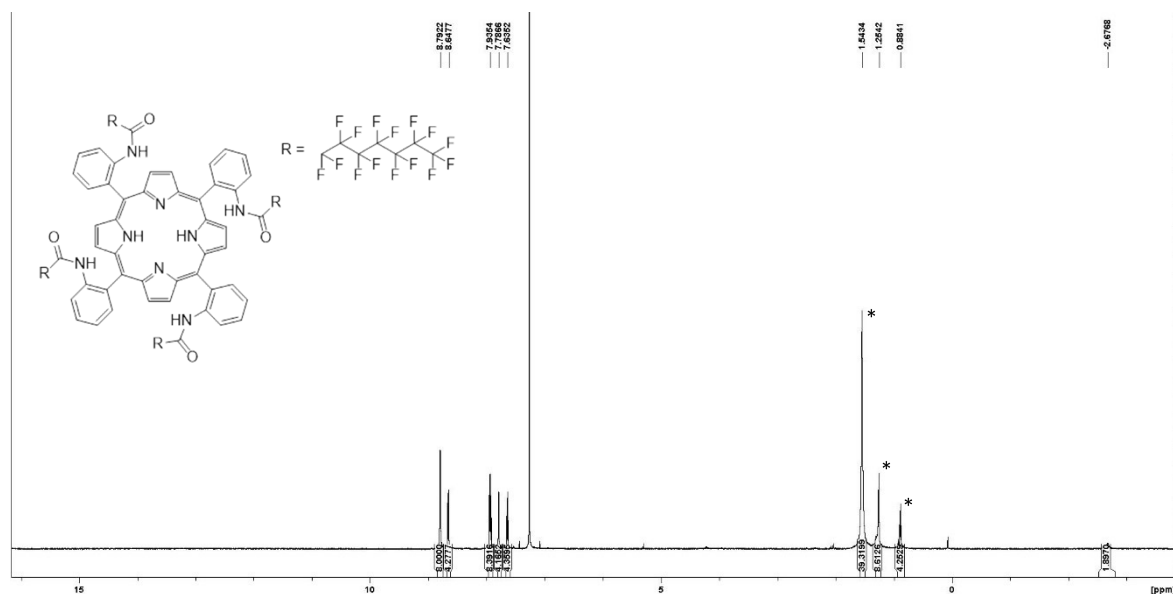


Figure S1: Host **1** ^1H NMR spectrum in CDCl_3 . Residual solvent peaks for petroleum ether (1.25 and 0.88 ppm) and water (1.54 ppm) have been noted with asterisks.

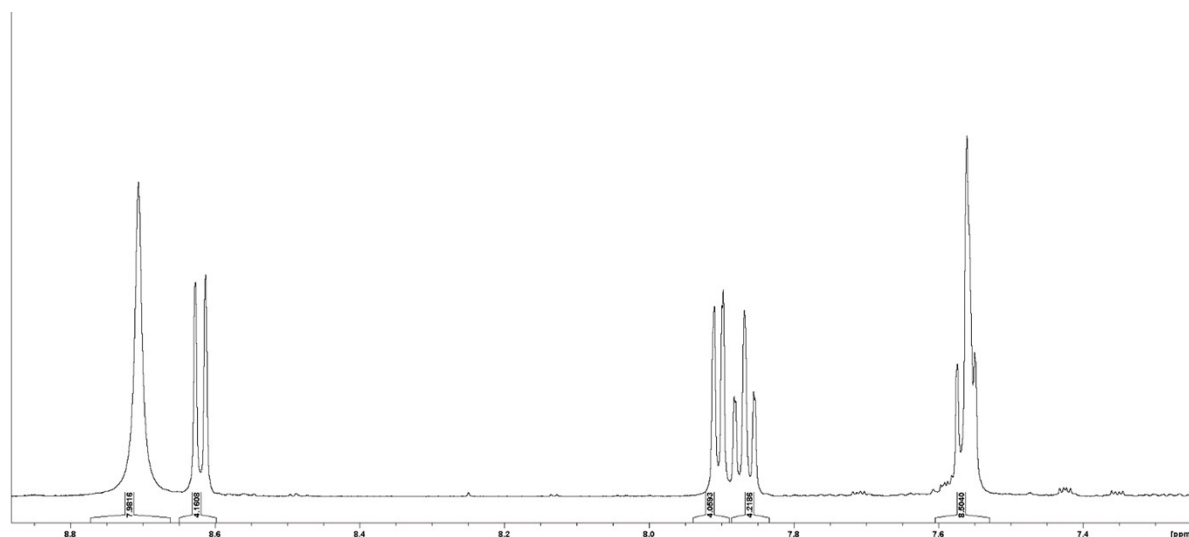


Figure S2: Host **1** ^1H NMR spectrum in CD_3OD (7.2 – 9 ppm). Host **1** showed aggregation effects in CDCl_3 , so this spectrum in deuterated methanol is included for clarity.

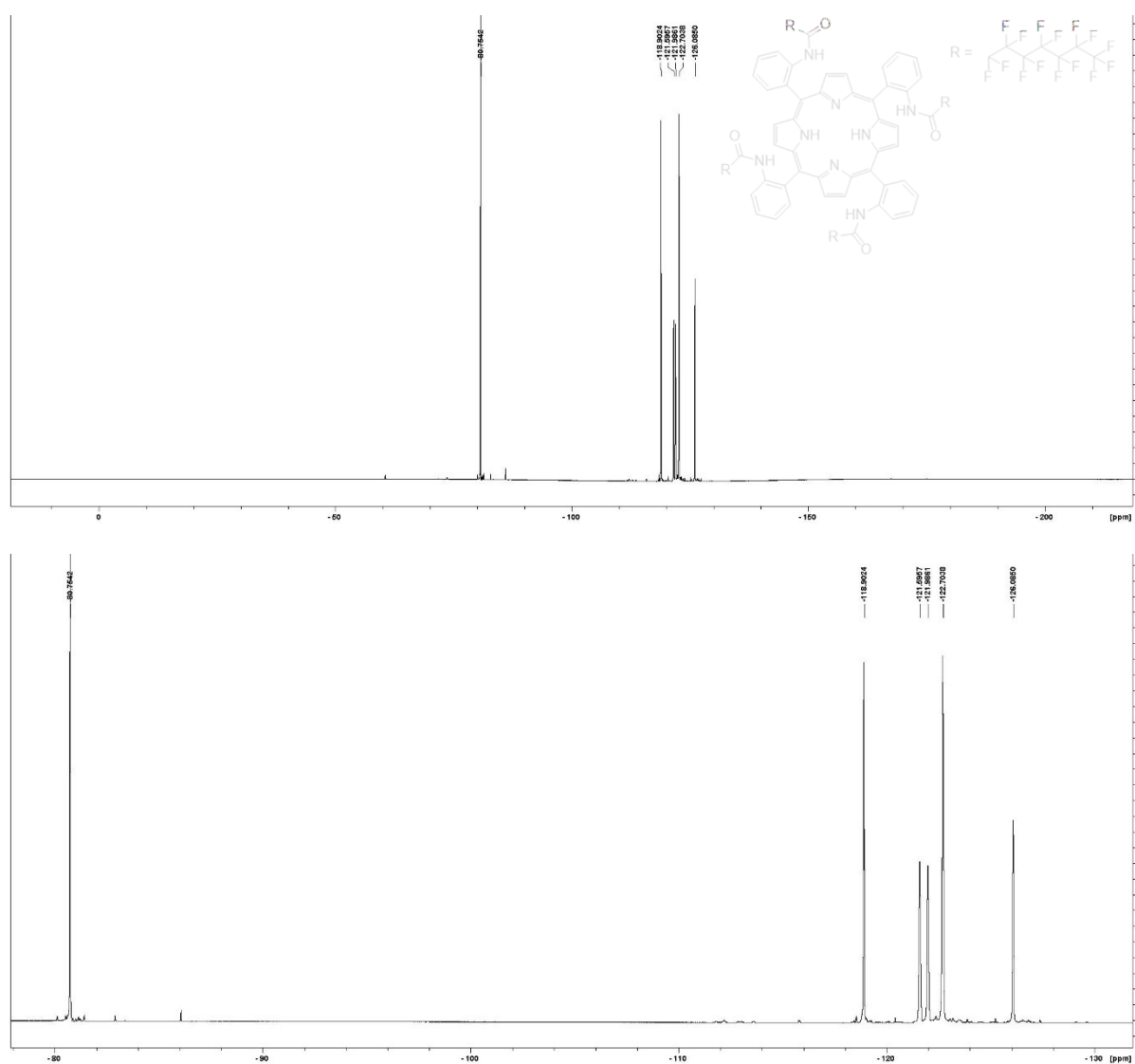


Figure S3: Host **1** ^{19}F NMR spectrum in CDCl_3 . Coincidental peaks occur at -122.7 ppm, full spectrum and region of interest (~ -90 – -130 ppm).

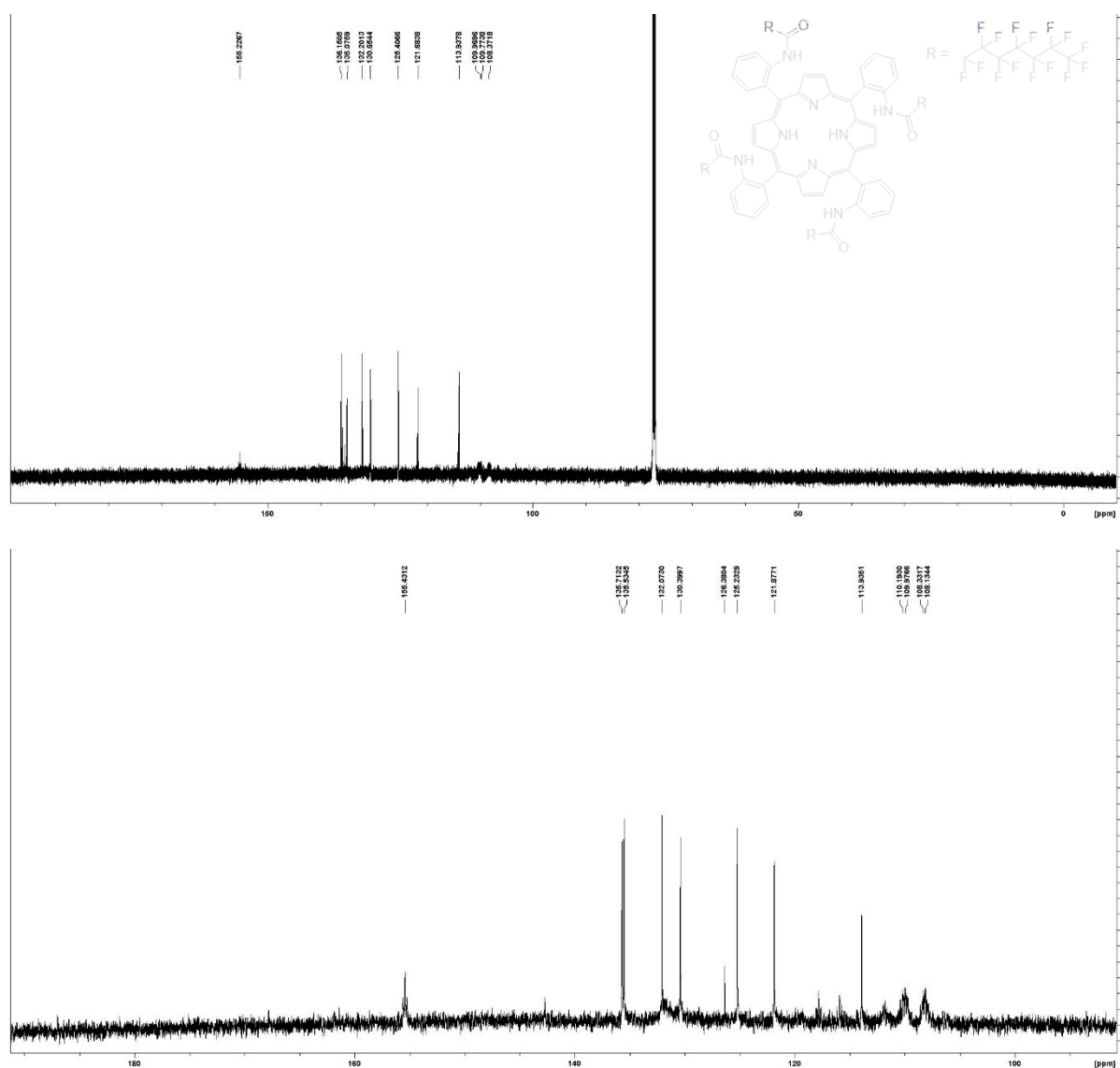


Figure S4: Host **1** ^{13}C NMR spectrum in CDCl_3 , full spectrum and region of interest ($\sim 100 - 190$ ppm).

S3– Mass Spectrometry

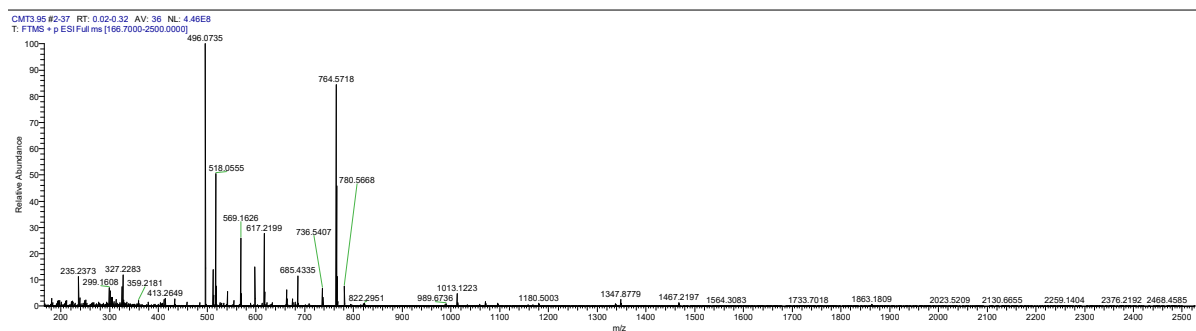


Figure S6: Low resolution mass spectrum of host **1**.

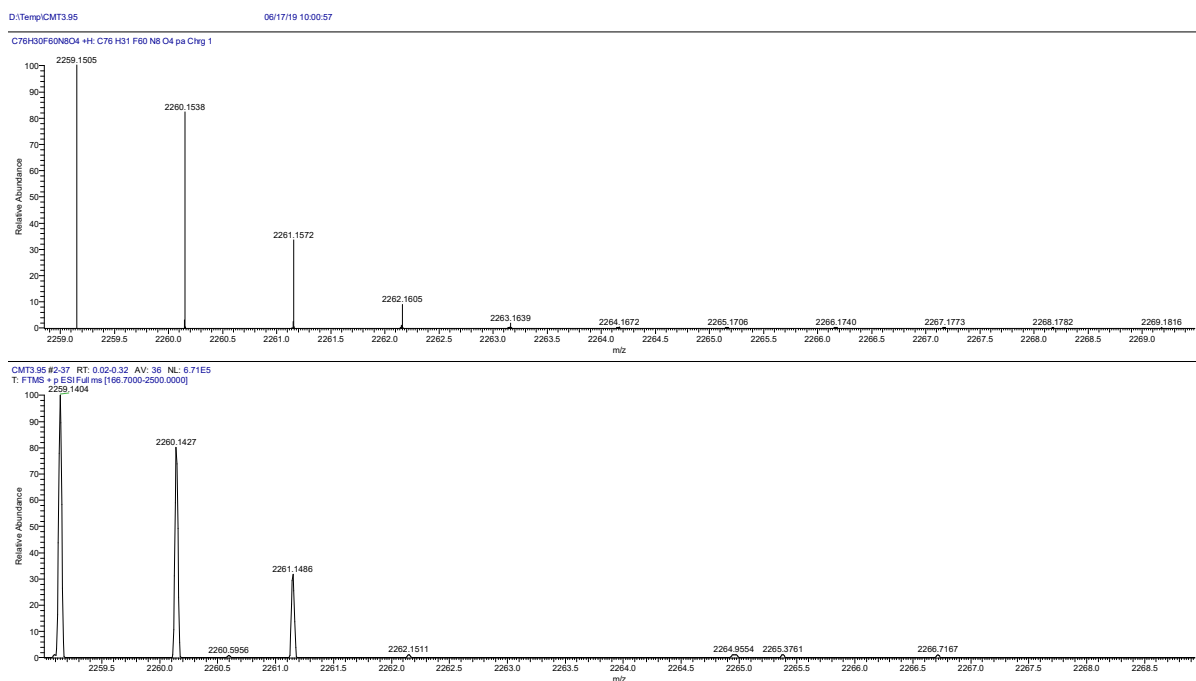


Figure S7: High resolution mass spectra of host **1**. FTMS + p ESI Full ms. m/z for $C_{76}H_{31}F_{60}N_8O_4$. Calcd 2259.1505, found 2259.1404

S4– Crystallography

General information X-ray crystallographic data for the structural determination of **1** were collected using synchrotron radiation ($\lambda = 0.71073 \text{ \AA}$) on the MX1 Beamline of the Australian Synchrotron.⁶ The structures were solved by intrinsic phasing methods with SHELXT⁷ and refined with SHELXL⁸ in OLEX2.⁹ Non-hydrogen atoms were refined with anisotropic displacement parameters. The perfluorinated moieties were observed to be disordered, and sections of these moieties were modelled over two positions of uneven occupancy. Carbon bound hydrogen atoms were visible in the diffraction map but were included at calculated positions and ride on the atoms to which they are attached. The positions of nitrogen bound hydrogen atoms were refined. Molecular graphics were produced with OLEX2. Crystallographic data were deposited with the Cambridge Crystallographic Data Centre (2080882).

Table S1: Crystallographic data for host **1**.

| | |
|--|--|
| Crystal data | |
| Chemical formula | $\text{C}_{76}\text{H}_{30}\text{F}_{60}\text{N}_8\text{O}_4 \cdot 0.5(\text{C}_6\text{H}_{14})$ |
| M_r | 2302.16 |
| Crystal system, space group | Triclinic, $P1$ |
| Temperature (K) | 100 |
| a, b, c (Å) | 13.920 (3), 14.710 (3), 22.500 (5) |
| α, β, γ (°) | 101.49 (3), 106.91 (3), 96.71 (3) |
| V (Å ³) | 4243.9 (17) |
| Z | 2 |
| Radiation type | Synchrotron, $\lambda = 0.71073 \text{ \AA}$ |
| μ (mm ⁻¹) | 0.20 |
| Crystal size (mm) | $0.05 \times 0.05 \times 0.05$ |
| Data collection | |
| Diffractionmeter | MX1, Australian Synchrotron |
| Detector | ADSC Quantum 210r |
| Absorption correction | — |
| No. of measured, independent and observed [$I > 2\sigma(I)$] reflections | 71163, 19307, 13675 |
| R_{int} | 0.062 |
| $(\sin \theta/\lambda)_{\text{max}}$ (Å ⁻¹) | 0.687 |
| Refinement | |
| $R[F^2 > 2\sigma(F^2)], wR(F^2), S$ | 0.049, 0.146, 1.04 |
| No. of reflections | 19307 |
| No. of parameters | 1767 |
| No. of restraints | 221 |
| H-atom treatment | H atoms treated by a mixture of independent and constrained refinement |
| $\Delta\rho_{\text{max}}, \Delta\rho_{\text{min}}$ (e Å ⁻³) | 0.48, -0.42 |

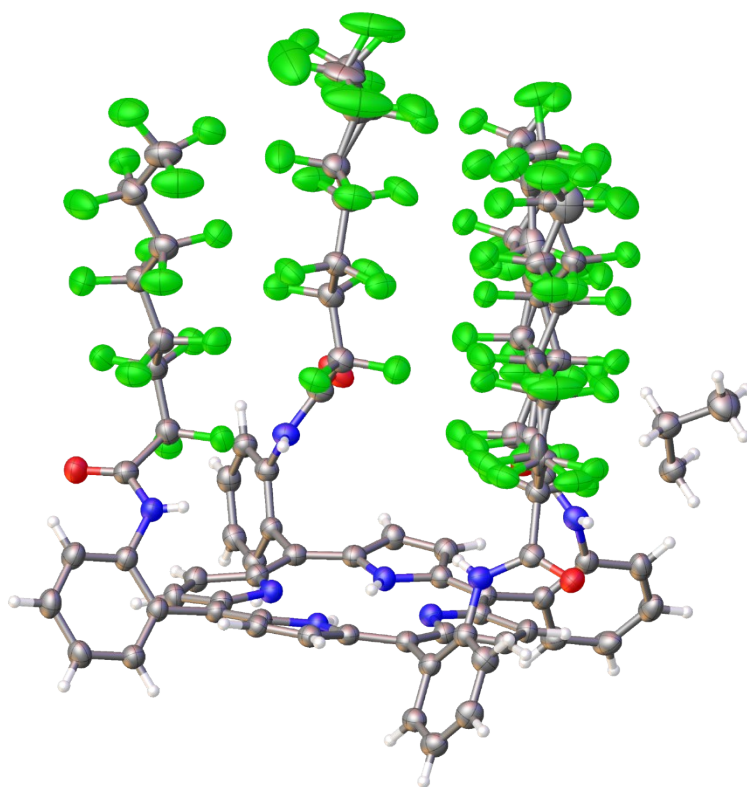


Figure S8: X-ray structure of **1** showing perfluorocarbon disorder and cocrystallised hexane. Ellipsoids are shown at 50% probability.

S5– UV-Visible Spectroscopic Analysis of Host Selectivity

Solutions of host **1** in dichloromethane were combined with 10 molar equivalents of guest molecules with some structural similarity to PFOA. Nonanoic acid and 1,2,4,5-tetrafluorobenzene were chosen as they approximated features of the PFOA molecule. A solution of host **1** (1.8×10^{-5} M) in dichloromethane was prepared. Three aliquots (2 mL) were transferred to glass cuvettes and a UV-visible spectrum was collected (red). To each sample, a solution of nonanoic acid (blue), 1,2,4,5-tetrafluorobenzene (purple), or TBAPFOS (orange), (1 mL, 3.6×10^{-4} M, 10 eq) in dichloromethane was added and analysed again. The absorbance showed no shifts or changes in intensity. There was a lowering in absorbance due to dilution upon guest addition, so the molar absorptivity coefficient has been used for regions of the spectra where the absorbance was below 2 absorbance units.

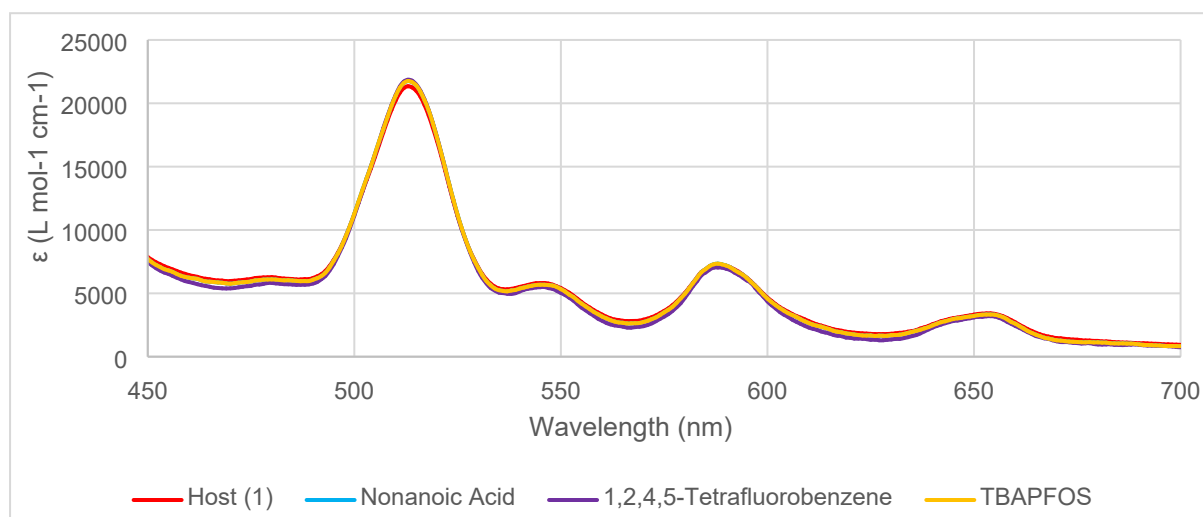


Figure S9: UV-Visible analysis of host **1** (red) when combined with 10 molar equivalents of nonanoic acid (blue), 1,2,4,5-tetrafluorobenzene (purple), and TBAPFOS (orange).

S6– UV-Visible Spectroscopic Analysis of Host – Guest Binding

The tetrabutylammonium (TBA) salts of anions were added in 10 molar equivalents to solutions of host **1** in dichloromethane. UV-vis spectroscopic analysis showed no significant change after the addition of TBA salts of Cl^- , Br^- , I^- , HSO_4^- , OAc^- , OH^- , F^- , and BF_4^- in contrast to a red shift in the Soret band (~ 27 nm) upon addition of the TBAPFO salt (Figure S10). The TBA salts for Cl^- , Br^- , I^- , HSO_4^- , OAc^- , PFO^- , and BF_4^- were added as solids, while the TBA salts for OH^- and F^- were added as aqueous solutions of known concentrations.

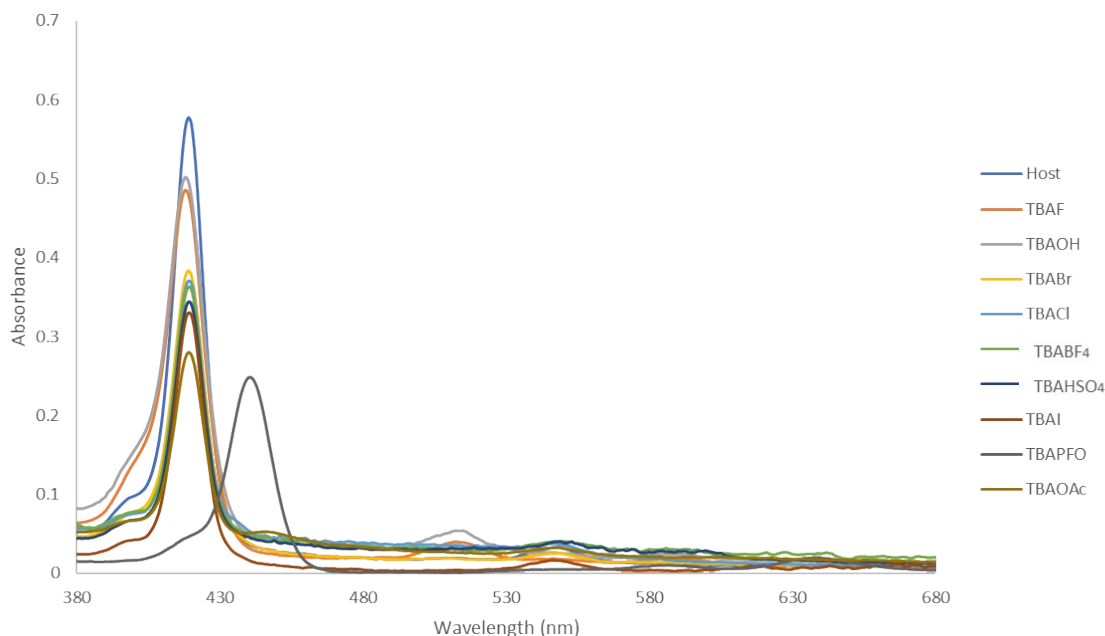


Figure S10: UV-vis spectra of host **1** (1×10^{-8} M) in dichloromethane combined with ten molar equivalents of a TBA salt.

A UV-visible spectroscopic host – guest titration was performed to assess binding interactions. This experiment was designed according to the methodologies presented in Thordarson's supramolecular titration guide.² A solution of host **1** in dichloromethane was prepared so that 0.6 mL of solution contained 6×10^{-10} mol of host **1**. A solution of guest (PFOA) was then prepared in the host solution so that 0.01 mL contained 1×10^{-11} mol of guest. Aliquots of guest in host solution were then added to host solution and sequentially analysed until a total of 6×10^{-10} mol of guest had been added (final volume 1.2 mL).

The data was then used to simulate binding isotherms using www.supramolecular.org. The data can be modelled using different algorithms. These experiments mainly used the Nelder-Mead (Simplex) method because it is the most robust option. The L-BFGS-B (quasi-Newtonian) method, which has higher importance/constraints on K value estimates, was also tested, and provided similar results. The binding mode of the host **1** was modelled as 1:1, 1:2 and 2:1 systems. Unsuccessful fitting and large error suggested the 1:2 and 2:1 binding modes were unreasonable estimations.

An example of the modelled data can be found here: <http://app.supramolecular.org/bindfit/view/e52777ac-5da6-4257-aff0-3d679b6ed9f0>

Table S2: Estimated K value using 0 – 15 guest equivalents and Nelder-Mead fitting parameters for 430 – 440 nm.

| K | K error (%) | SSR | Datapoints fitted | Params fitted | H coeffs | HG coeffs | Raw coeffs 1 | Raw coeffs 2 |
|------------|-------------|------------|-------------------|---------------|----------|------------|--------------|--------------|
| 3030126.75 | 16.3695692 | 8.19765268 | 198 | 12 | 68900 | 2678473.12 | 68900 | 2678473.12 |
| | | | | | 77500 | 2627310.76 | 77500 | 2627310.76 |
| | | | | | 88700 | 2548145.9 | 88700 | 2548145.9 |
| | | | | | 102800 | 2438858.38 | 102800 | 2438858.38 |
| | | | | | 120600 | 2291993.1 | 120600 | 2291993.1 |
| | | | | | 144600 | 2116082.96 | 144600 | 2116082.96 |
| | | | | | 175500 | 1917852.92 | 175500 | 1917852.92 |
| | | | | | 213200 | 1717657.73 | 213200 | 1717657.73 |
| | | | | | 260700 | 1526845.91 | 260700 | 1526845.91 |
| | | | | | 318400 | 1353615.81 | 318400 | 1353615.81 |
| | | | | | 389300 | 1199058.35 | 389300 | 1199058.35 |

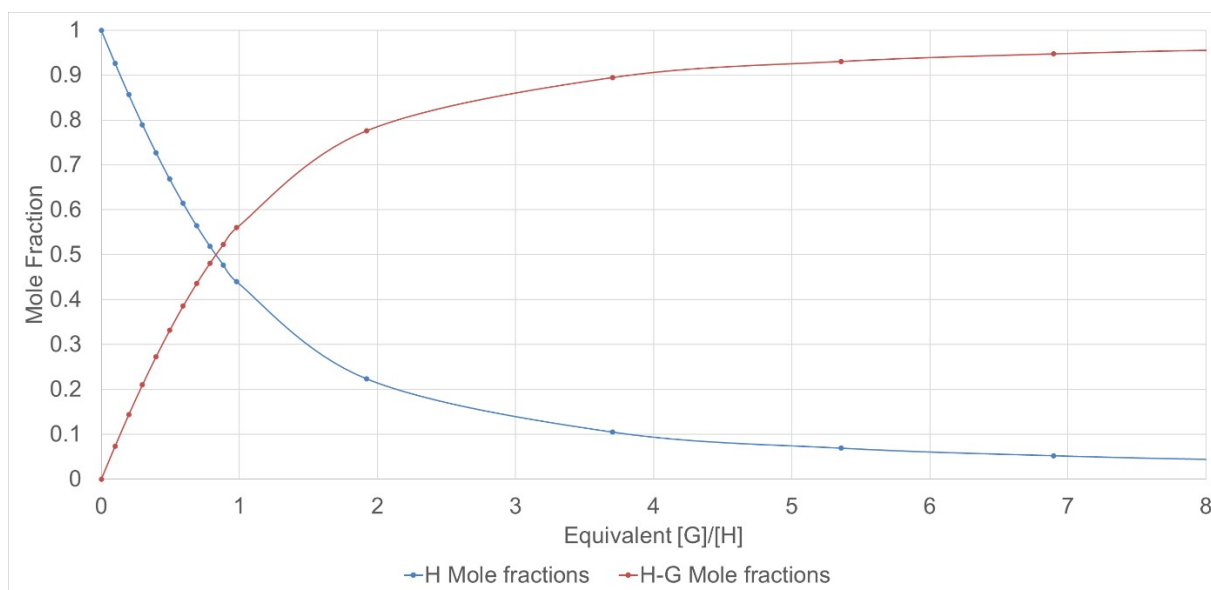


Figure S11: Mole fraction plot for host 1 plus PFOA titration.

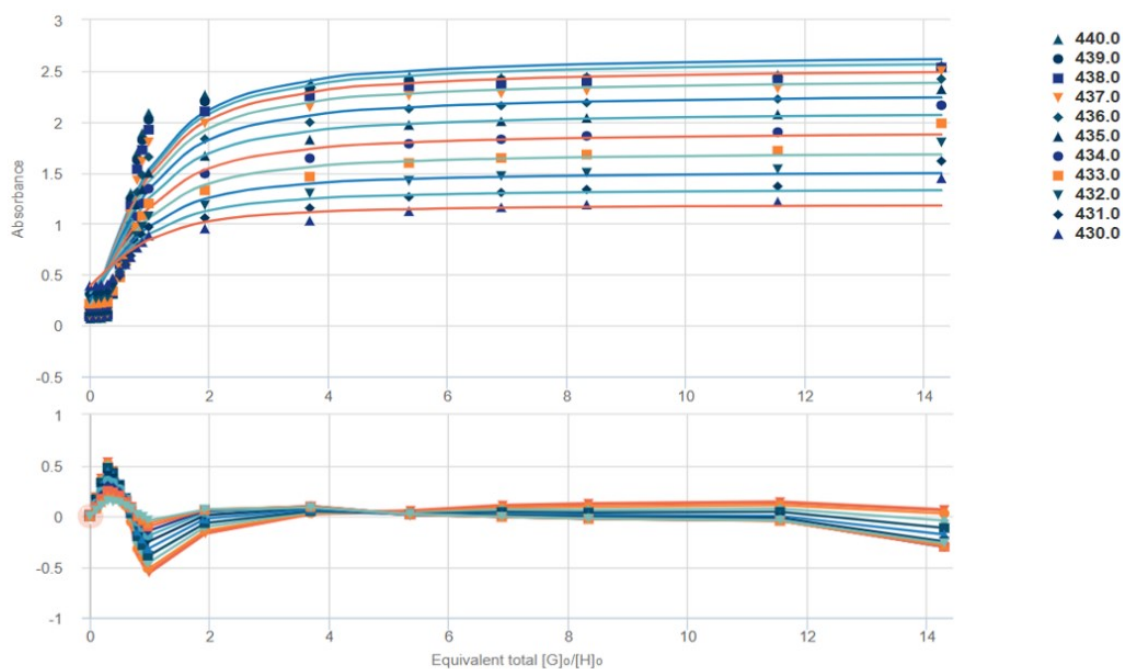


Figure S12: Absorbance across a range of modelled wavelengths for the molar ratio of host **1** and PFOA (equivalent $[G]/[H]$), with residuals.

This experiment was repeated using TBAPFO as a guest. An example of the modelled data can be found here: <http://app.supramolecular.org/bindfit/view/0d6d2449-7129-4df8-b0cc-c30f206d427d>

Table S3: Estimated K value using 0 – 10 guest equivalents and Nelder-Mead fitting parameters for 515 – 508 nm.

| K | K error (%) | SSR | Datapoints fitted | Params fitted | H coeffs | HG coeffs | Raw coeffs 1 | Raw coeffs 2 |
|------------|-------------|------------|-------------------|---------------|------------|------------|--------------|--------------|
| 2085552.83 | 10.1700281 | 0.00620603 | 112 | 9 | 138733.333 | 36646.6559 | 138733.333 | 36646.6559 |
| | | | | | 140866.667 | 36825.6473 | 140866.667 | 36825.6473 |
| | | | | | 141600 | 36828.3721 | 141600 | 36828.3721 |
| | | | | | 140800 | 36395.8452 | 140800 | 36395.8452 |
| | | | | | 138133.333 | 36217.7127 | 138133.333 | 36217.7127 |
| | | | | | 133800 | 36094.2057 | 133800 | 36094.2057 |
| | | | | | 128333.333 | 36120.4665 | 128333.333 | 36120.4665 |
| | | | | | 122266.667 | 35804.0569 | 122266.667 | 35804.0569 |

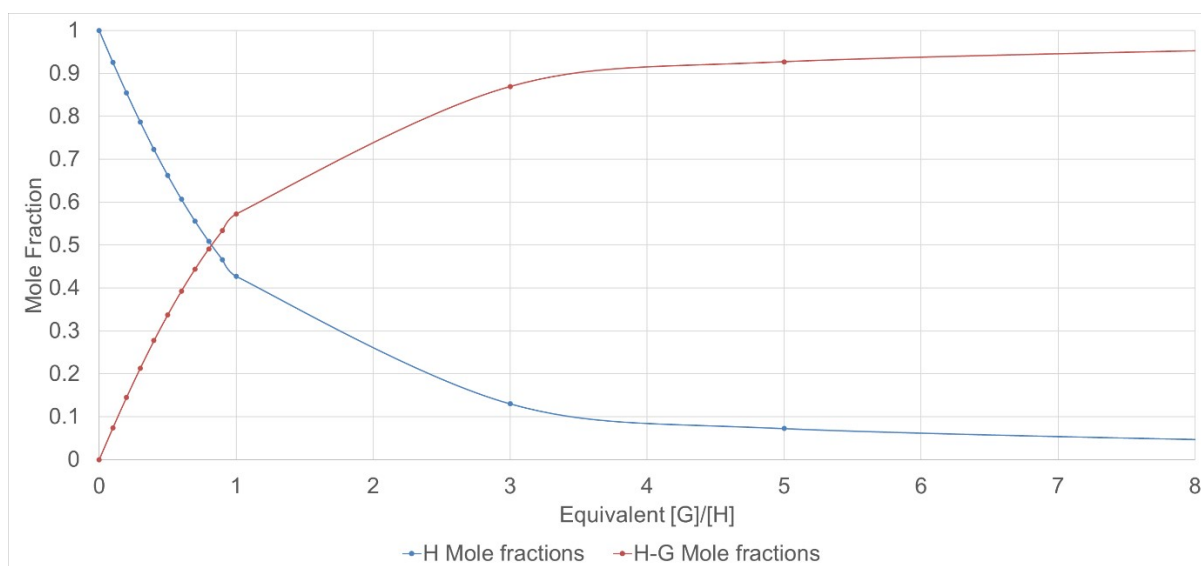


Figure S13: Mole fraction plot for host **1** plus TBAPFO titration.

S7– Biphase Extraction Experiments

Preliminary biphasic extractions were performed using high concentrations of aqueous PFOA to gauge the visibility of color change in the host molecule **1** at different concentrations. A concentrated stock solution of host **1** (2.2×10^{-2} M) in dichloromethane was prepared and serially diluted. Aliquots of each concentration were then combined with an aqueous PFOA solution (114 ppm, 2.75×10^{-4} M) in small vials. The vials were capped and agitated. Although a color change was easily discernible across the range, more concentrated host solutions are significantly darker, which can make the green color less visible by eye (Figure S14).

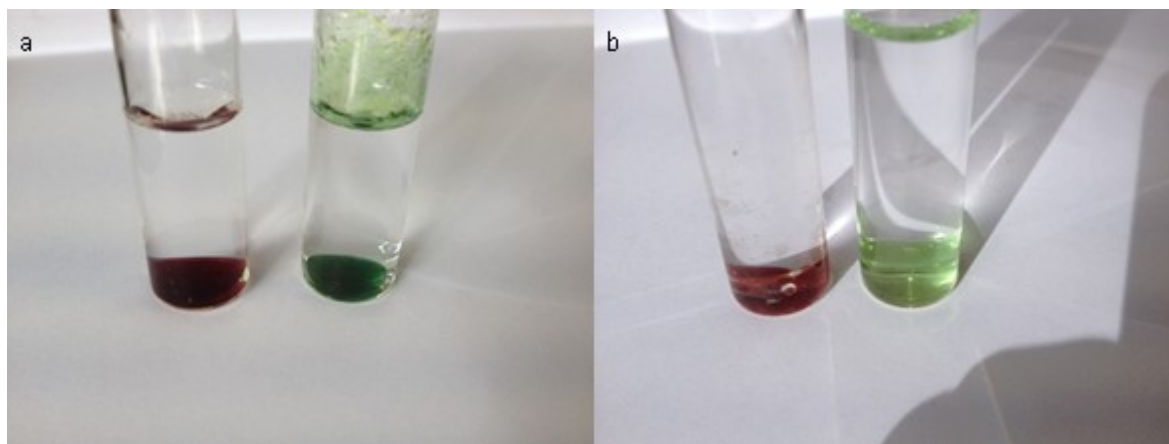


Figure S14: (a) Red solution of host **1** (2.2×10^{-2} M) in dichloromethane with water, green solution of host **1** in dichloromethane with aqueous PFOA (114 ppm, 2.75×10^{-4} M). (b) Red solution of host **1** (5.5×10^{-3} M) in dichloromethane with water, green solution of host **1** in dichloromethane with aqueous PFOA (114 ppm, 2.75×10^{-4} M).

To detect PFOA by eye at lower concentrations, it is preferable to have the number of moles of PFOA in excess relative to the host molecule **1**. A solution of host **1** in dichloromethane (5 mL, 6.2×10^{-6} M) was combined with an aqueous solution of PFOA (3 ppm, 7.23×10^{-6} M, 500 mL) and agitated (Figure S15). The organic phase was then collected and analysed using UV-visible spectroscopy. A solution of host **1** in dichloromethane (5 mL, 6.2×10^{-6} M) is combined with a water sample (500 mL) and collected to be analysed using UV-visible spectroscopy as a control.

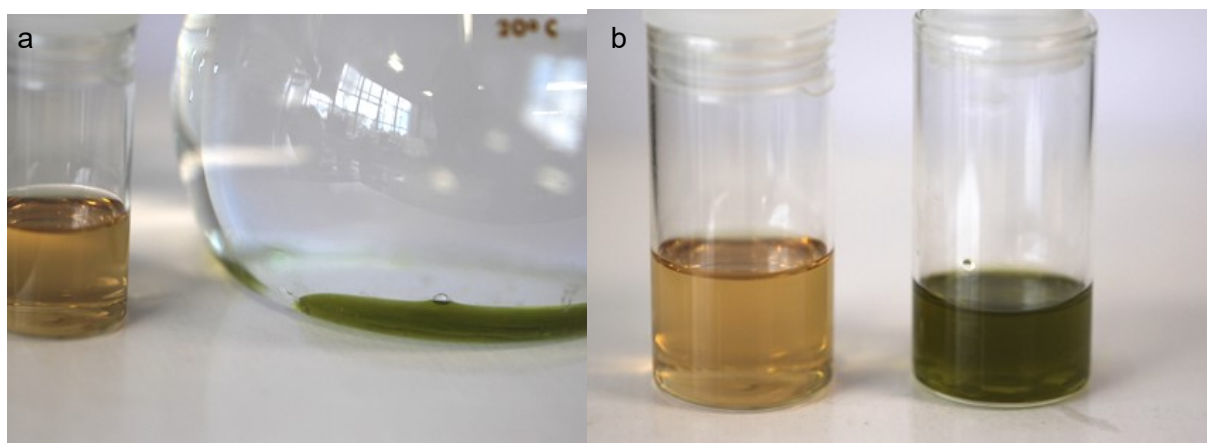


Figure S15: (a) Control solution of host **1** in dichloromethane (left), and host **1** when combined with a 500 mL aqueous PFOA sample (right). (b) Control solution of host **1** (left) next to a collected organic phase of host **1** from an aqueous PFOA extraction for direct comparison (right).

The $1 \text{ } \square \text{ } \text{PFO}^-$ binding is evidenced by the increase of a peak at ~ 650 nm (Figure S16). This region is analysed because the absorbance at these concentrations is below 2 absorbance units, and performing further dilutions would potentially result in increased sorption of PFO^- to the volumetric glassware. When trialling “shake”

extractions at significantly lower concentrations, polypropylene tubes were used when possible, to prevent loss of PFO⁻ to the internal surfaces of the vessel.

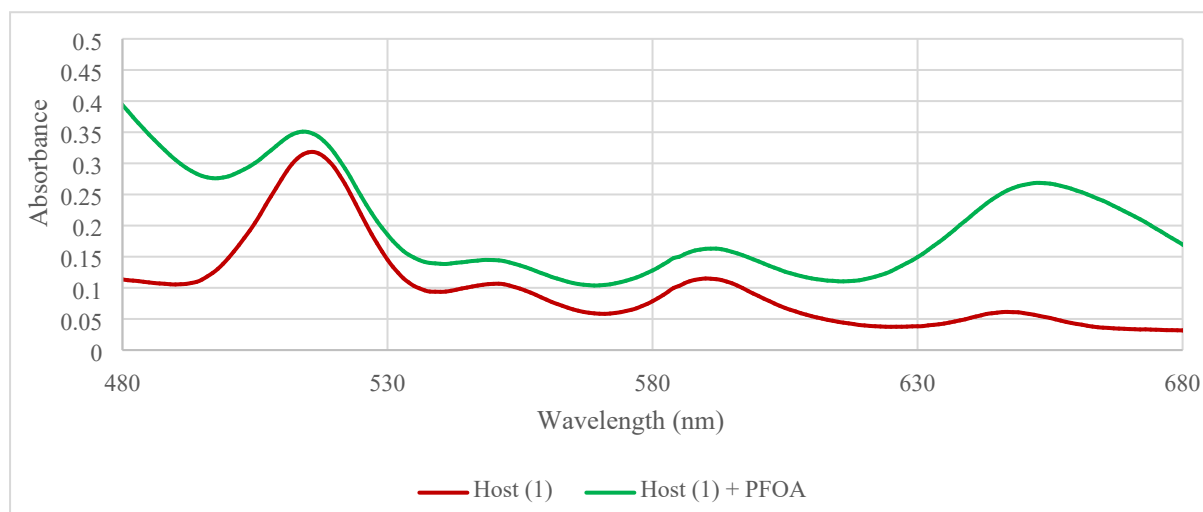


Figure S16: UV-Visible analysis of aqueous PFOA biphasic extraction. Control solution of host **1** (6.2×10^{-5} M) in dichloromethane (red), and host **1** (6.2×10^{-5} M, 5 mL) when combined with an aqueous PFOA sample (3 ppm, 7.23×10^{-6} M, 500 mL) (green).

S8– Soil Extraction Procedures

Spiked soil and control soil was prepared according to previously reported methods.^{3-5, 10} A concentrated solution of host **1** is prepared and added to the filtered solvent (dichloromethane). Only microlitres of host **1** solution is required, which also prevents significant dilution of the extracted PFOA. An excess of PFOA to host **1** provided the most vivid color change. When possible, polypropylene tubes were used for the “shake” extraction step, but the filtration and analysis process required the use of nonideal materials. Glass frits, cotton wool and Whatman filter papers were used depending on masses of dirt, soil composition and solvent volumes.¹¹

Example procedure: Triplicate soil samples (10 g) of PFOA spiked (15 ppm) and control dirt were weighed into small glass vials. To each vial, dichloromethane (20 mL) was added. The vial was capped, agitated, and left to settle briefly so the color of the solvent could be noted. The solutions were then filtered over cotton wool using a ceramic Hirsch funnel, and the dichloromethane filtrate was placed in a glass vial. To each dichloromethane solution, the host molecule **1** in dichloromethane (8.85×10^{-4} M, 10 μ L) was added. The vials were then photographed (Figure S17). Aliquots of the dichloromethane host **1** solutions were taken and diluted by 50% to be analysed using UV-visible spectroscopy. The Soret band of the host **1** shifts but is above an absorbance of 2, so the increase in the ~ 660 nm region is also monitored, as it is expected to change for the formation of the **1**-PFOA complex (Figure S18).

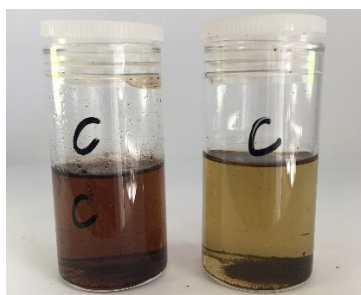


Figure S17: The dichloromethane post soil extraction, filtering, and the addition of host **1** (8.85×10^{-4} M, 10 μ L). The darker red vial (left) is the control sample, the lighter green vial (right) is from the extraction of PFOA spiked soil (15 ppm).

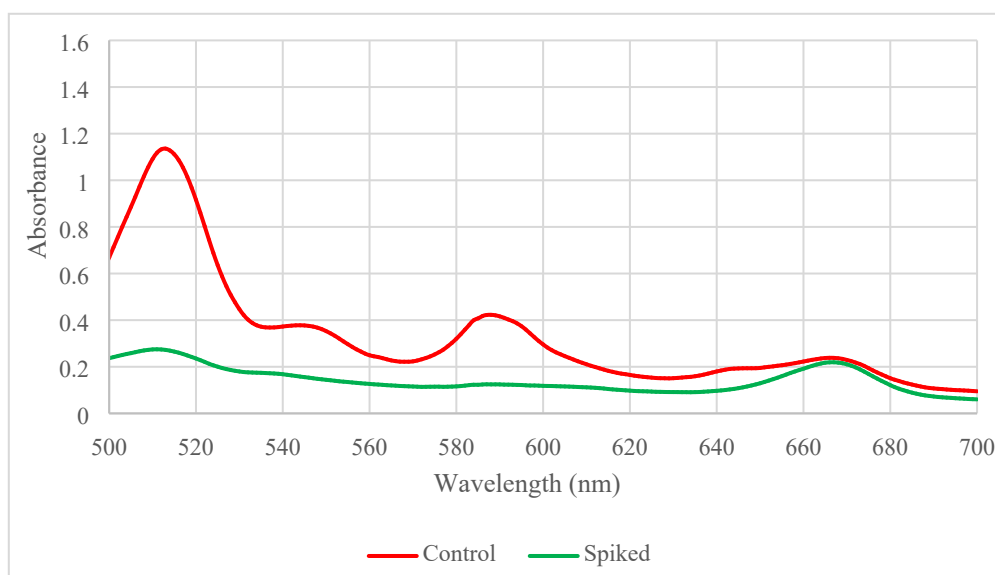


Figure S18: UV-Visible comparison of control and spiked soil extractions (50% dilution). The host **1** solution (red) from a control soil extraction and the host **1** solution (green) collected from PFOA spiked soil (15 ppm).

Reference

1. B. L. Bales and R. Zana, *Langmuir*, 2004, **20**, 1579-1581.
2. P. Thordarson, *Chem. Soc. Rev.*, 2011, **40**, 1305-1323.
3. U. C. Brinch, F. Ekelund and C. S. Jacobsen, *Appl. Environ. Microbiol.*, 2002, **68**, 1808-1816.
4. S. Swami, presented in part at the Hands on Soil Testing, 10.13140/RG.2.2.32675.48164, 2020.
5. G. L. Northcott and K. C. Jones, *Environ. Toxicol. Chem.*, 2000, **19**, 2409-2417.
6. N. P. Cowieson, D. Aragao, M. Clift, D. J. Ericsson, C. Gee, S. J. Harrop, N. Mudie, S. Panjekar, J. R. Price, A. Riboldi-Tunnicliffe, R. Williamson and T. Caradoc-Davies, *J Synchrotron Radiat.*, 2015, **22**, 187-190.
7. G. M. Sheldrick, *Acta Cryst.*, 2015, **C71**, 3-8.
8. G. M. Sheldrick, *Acta Cryst.*, 2015, **A71**, 3-8.
9. O. V. Dolomanov, L. J. Bourhis, R. J. Gildea, J. A. K. Howard and H. Puschmann, *J. Appl. Crystallogr.*, 2009, **42**, 339-341.
10. A. Halasz, J. M. Bayona and J. Hawari, in *Comprehensive Analytical Chemistry*, Elsevier, 2002, vol. 37, pp. 895-918.
11. S. Lath, E. R. Knight, D. A. Navarro, R. S. Kookana and M. J. McLaughlin, *Chemosphere*, 2019, **222**, 671-678.